HEFAT2007
5th International Conference on Heat Transfer, Fluid Mechanics and Thermodynamics
1 – 4 July 2007, Sun City, South Africa
Paper number: BF1

Numerical and Experimental Evaluation of the Time-Variant Flow Field in a Single-Blade Centrifugal Pump

Benra F.-K.*, Dohmen H. J.
*Author for correspondence
University of Duisburg-Essen,
Faculty of Engineering Sciences,
Institute of Energy and Environmental Engineering,
P. O. Box 1629,
D-47048 Duisburg, Germany,
E-mail: friedrich.benra@uni-due.de

ABSTRACT

In this contribution the time-variant flow in a single-blade pump is evaluated by numerical and experimental methods. In a numerical approach the three-dimensional, viscous, unsteady flow field in the complete pump has been achieved by solving the unsteady Navier-Stokes equations (URANS) with different commercial solvers in a wide range of pump operation. From the calculated periodic flow field the hydrodynamic forces resulting from the time-variant pressure field and viscous stresses were determined for a complete impeller revolution. To validate the results of the numerical simulations a test rig was used to conduct some measurements in the pump. First of all the velocity field inside the pump was investigated by using the Particle Image Velocimetry. A good agreement between the velocity fields obtained by numerical simulations and by measurements has been achieved. In a second step the transient hydrodynamic forces of the pump were measured by acquisition of the appropriate forces acting on the bearings of the pump rotor during operation. The measurements of the hydrodynamic forces match the results of the numerical simulations very well. In particular, the good qualitative agreement suggests that predicting the transient flow in (single-blade) centrifugal pumps utilizing a Navier-Stokes (URANS) solver, is a reliable method to determine the time-variant hydrodynamic forces, which are decisive for the vibrations of the pump.

INTRODUCTION

Raw sewage water typically contains large amounts of solids and fibers. The transport of water comprising such impurities can preferably be done by using centrifugal pumps which have a special impeller geometry, in order to avoid operational disturbances by clogging. Non-clogging sewage water pumps normally are single-stage pumps which are equipped with impellers featuring a small number of impeller blades. Single-blade impellers provide the largest cross sections of the flow channel and are therefore most effective avoiding clogging. But there are also disadvantages which occur during pump operation, because the periodic unsteady flow in the impeller is interacting with the casing and during rotation of the impeller a strongly unequal pressure field at the perimeter of the volute is produced. The time-variant flow in such pumps results in periodic unsteady flow forces which affect the impeller and which produce strong radial deflections of it [1-3]. The periodic bending of the pump shaft aligned with the deflections arouses extensive alternating load to the material and often leads to a failure.

The examination of the flow field in pumps in general can be achieved by analytical, numerical and experimental methods. Because of the complexity of the pump geometry the flow field normally has strong variations of all parameters in all three coordinate directions. Additionally, due to the rotating impeller the flow is strictly transient. The known analytical methods are unable to predict such a flow field with the required accuracy. Numerical methods solving the Reynolds Averaged Navier-Stokes equations have been developed to powerful tools in the past decade. Combined with the available computer hardware, which also has been strongly enhanced in the past, substantial numerical solutions for complex flow fields can be realized in a time-consuming and cost saving way even for time-variant flows. But the question which has to be placed is: What about the quality of the results and how reliable are the solutions? This question only can be answered when the results of the fluid mechanical problem are known a priori or if not, by using a complete different examination method for validation. This leads to the experimental evaluation methods, which in most cases are more costly and time-consuming than the numerical methods. But they can show the real behavior because nearly no assumptions and simplifications must be accomplished. A disadvantage of the experiments is that for the

evaluation of divers flow parameters often completely different tests are necessary.

In this contribution the time-variant flow in a single-blade pump is evaluated by numerical and experimental methods. To validate the results of the numerical simulations which have been done using different commercial flow solvers a test stand has been used to conduct some measurements in the pump. The velocity field inside the pump can be beneficially investigated by using the Particle Image Velocimetry [4, 5]. At the same time the transient hydrodynamic forces of the pump were measured by acquisition of the appropriate forces acting on the bearings of the pump rotor during operation. The examination of the periodic velocity field inside the pump and the indirect evaluation of the pressure field around the impeller by measuring the hydrodynamic forces required completely different investigation methods but could be executed at the same time.

NOMENCLATURE

Arabic letters

b	mm	blade height
D	mm	diameter
F	N	force
H	m	delivery head
K	mm	free ball passage
n	rpm	shaft speed
n_q	rpm	specific speed
Q	m^3/h	volume flow rate
u	m/s	circumferential velocity
v	m/s	velocity in absolute frame
x, y, z	m	Cartesian coordinates (relative frame)

Greek letters

α	deg	angle of circumferential evaluation line
β	deg	blade camber line angle
φ	deg	angle of rotation
Θ	deg	blade wrap angle
ρ	kg/m^3	fluid density
ξ, ψ, ζ	m	Cartesian coordinates (absolute frame)

Subscripts

amb	ambient
ann	annular
des	design
imp	impeller
s	suction
rel	relative
ref	reference
2D	2-dimensional

NUMERICAL INVESTIGATIONS

A numerical determination of the flow in a centrifugal pump requires a model, in which beside the outer boundaries of the computing area also the spatial discretization of the flow area is described. On the basis of a volume model of the pump in the parametric CAD system ProEngineer the flow area was discretized by a block-structured computing grid with the grid generator Ansys ICEM CFD. Since neither the impeller nor the casing possessed a plane of symmetry, a complete meshing of the fluid volume for all components was necessary. The grid of the impeller contained 68 blocks with approximately 884000 grid points, while for the casing 27 blocks with approximately 338000 grid points were generated. The grids of both the hub and the shroud side chambers between the impeller discs and the casing walls were created together with the grid of the impeller. In this way the leakage flow from pressure side to suction side has been incorporated in the analysis. The grids of the impeller and the casing were attached to each other by a general interface at a cylindrical surface, which allows the grid of the impeller to rotate in the casing (sliding mesh). The independence of the solutions from the number of grid nodes has been proven by simulating the flow field with a larger number of grid nodes. The non-dimensional distance of the first grid nodes to the wall (y^+-values) was below 100 in the complete flow field. The numerical simulations have been accomplished with different solvers, different discretization schemes and different boundary conditions but with the same turbulence model (k-ω-SST). For the first investigations the solver CFX-Tascflow was used. Because of achieving a better support, later we switched to CFX10 using different boundary conditions in order to check the former results.

CFX-TASCflow: Second order spatial discretization, first order backward time discretization. Inlet boundary conditions: mass flow rate and direction of absolute velocity. Outlet boundary condition: area averaged static pressure.

Ansys CFX10: Second order spatial discretization, second order backward time discretization. Inlet boundary conditions: total pressure and direction of absolute velocity. Outlet boundary condition: mass flow rate.

In figure 1 the numerical model of the single-blade pump is depicted showing the boundary conditions used for the CFX10 code. In addition some details of the computational grid at the leading edge and at the trailing edge are given. This numerical model will be referred to as “open loop” in the following. More information about the numerical simulation procedures can be taken from [6] for example.

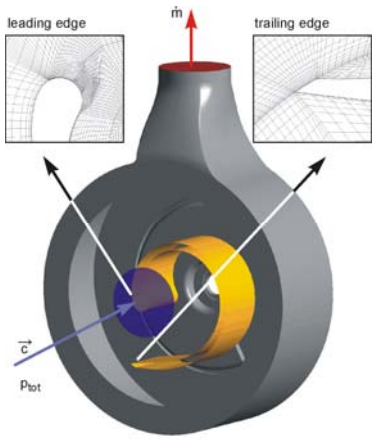

Figure 1: Numerical model of single-blade pump

The results of the first simulations with the NS-solver TASCflow are shown in figure 2 for the open loop calculation for four operating points in the rotating coordinate system. The figure shows the results of the tenth impeller revolution after starting the simulation. Beside the design point two part load operating points (50% of Q_{des} and 75% Q_{des}) and one overload operating point (125% of Q_{des}) have been evaluated. The calculated pump head overestimated the measured head by about 5% for all four duty points. The hydrodynamic forces have been divided by a reference force in order to make them non-dimensional (F^*). The reference force is given by equ. 1:

$$F_{ref} = \frac{\rho}{2} \cdot u_2^2 \cdot b_2 \cdot \frac{D_2}{2} \qquad (1)$$

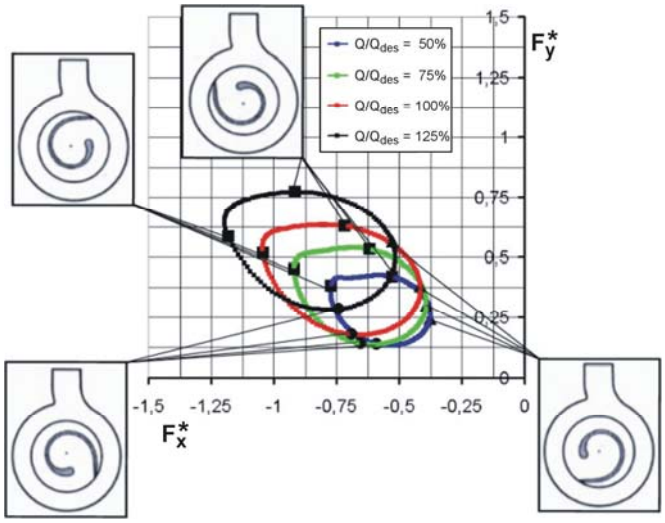

Figure 2: Calculated radial forces for 4 operating points

The components of the hydrodynamic forces perpendicular to the shaft axis (x and y co-ordinate) cause a radial deflection of the pump shaft. So they are called the radial components of the hydrodynamic forces. Both force components show a strong variation during one impeller revolution but have the same behavior for all 4 operating points: They appear in the 3rd quadrant of the coordinate system and the shape is similar for all operating points. Obviously the amplitudes of both force components increase with increasing flow rate which is a little bit curious in consideration of the decreasing head of the pump. Later simulations with the NS-solver Ansys CFX10 using the same computing grid but different boundary conditions showed nearly the same results.

To answer the question if this behavior can be attributed to the constant boundary conditions (pressure and mass flow) given at the inlet flange and at the outlet flange of the pump, a new simulation model has been developed for this pump. This new model treated the pump as a closed loop. The same spatial discretization has been used for the pump, but to overcome the constant flow rate at the outlet flange of the pump a pipe has been attached at the pressure flange which includes a loss module. Behind the loss module the pipe meets the inlet flange of the pump building a closed loop (see figure 3). For this closed loop model no mass flow must be given as a boundary condition. The mass flow of the pump has been calculated during the simulation and it varied with the impeller turning angle. Conducting preliminary transient simulations the time averaged mass flow has been fitted by varying the loss coefficient of the loss module in several approaches. When the computed time-averaged mass flow had the same amount than the flow rate under investigation the loss coefficient has been regarded as well adjusted. The simulations for this "closed loop" have also been conducted with the NS-solver Ansys CFX10.

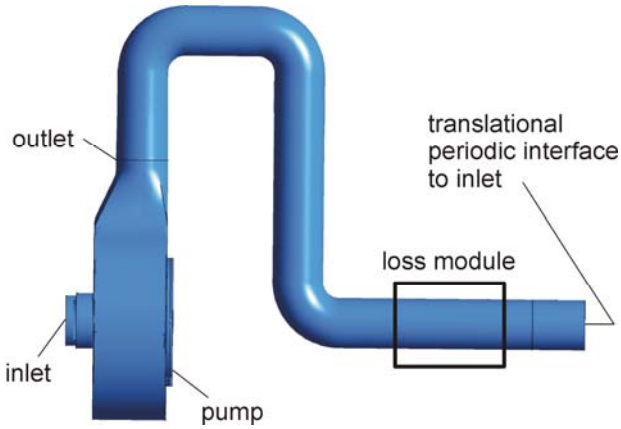

Figure 3: Scheme of the closed loop model for numerical simulation

In figure 4 the results for the design operating point of this calculation are compared to the open loop calculation with CFX10. The non-dimensional components of the forces are presented in the absolute coordinate system as orbit curves. As mentioned before, the calculations for the open loop with the codes TASCflow and CFX10 show nearly the same results. The difference between the two simulations appears predominantly in the 2nd and 3rd quadrant of the coordinate system. The ξ-components of the forces differ up to 20 percent between the closed loop simulation and the open loop simulation. But as the ξ-components of the forces in the 1st and in the 4th quadrant are nearly the same, it is clear that the variation of the forces during one impeller revolution is stronger for the closed loop compared to the open loop.

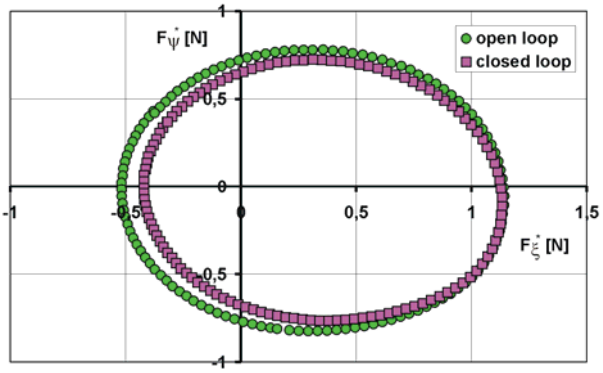

Figure 4: Comparison of open and closed loop force orbits

EXPERIMENTAL INVESTIGATIONS

To validate the results obtained by the different CFD methods, measurements have been accomplished at a test stand which originally had been constructed under the guidance of Prof. Siekmann, Technical University of Berlin [7]. In figure 5 a schematic view of the test facility is shown. The test stand contains a vertical arranged submersible single-blade pump which is powered by an electric motor with constant speed. The motor drives a cardan shaft which is connected to the pump shaft. This pump was particularly designed for that test facility in order to measure the velocity fields in the pump by optical methods. So the single-blade pump under examination here was completely manufactured out of transparent plastic, and it is characterized by the design operating conditions and geometric design parameters given in Table 1. The angle β_1 at the leading edge of the blade is very small and the wrap angle of the blade is bigger than Θ = 330 deg. This combines to a maximum free cross-section of the impeller flow channel K = 70 mm at the outlet, which is also called the "free ball passage" of the pump.

Operating conditions		Design variables			
Q	146.2 m^3/h	D_{ann}	380 mm	β_1	9 deg
H	12.5 m	D_{imp}	240 mm	β_2	35 deg
n	1450 rpm	D_s	100 mm	Θ	332 deg
n_q	43.8 rpm	b	80 mm	K	70 mm

Table 1: Design parameters of test pump

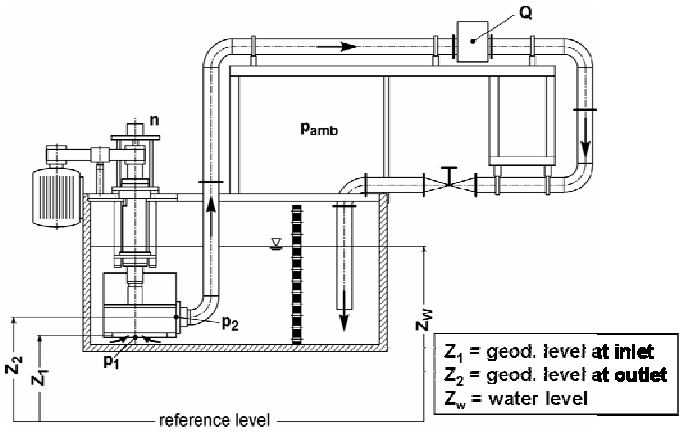

Figure 5: Test rig for submersible pump

As the holding tank (about $3{,}5m^3$ of pure water) is also equipped with transparent plastic windows, optical access for the PIV-system is provided. The PIV system has been arranged outside the holding tank. The ray of the Nd-Yag-Laser system has been extended by optical lenses to a light sheet of about 4 mm thickness which is sent from outside through the optical access to illuminate the particles in the water. The light source was a 20 Hz Dual Nd-Yag-Laser with a maximum pulse energy of 120 mJ per beam and the images have been taken by a CCD camera with a number of 1024 to 1280 pixels and a resolution of the grey scale of 8 bit. The CCD-camera has been mounted at a 2D traverse system below the water tank and the traverse system has been placed at a lift table to permit movement of the camera also in the vertical coordinate direction. The view of the used CCD-camera was 57 x 72 mm^2 which was much smaller than the plane of the complete pump. So the complete view under investigation has been divided into 35 single views. Pictures of each part view have been repeated 20 times for the same impeller position in order provide a statistical average. An initial impeller position has been indicated by an inductive impulse sensor. Outgoing from this signal a certain time delay has been calculated to achieve measurements for a special impeller position. In order to achieve a complete view of the flow inside the pump, all part views have been combined after the averaging process.

In figure 6 the measured velocities in the absolute coordinate system are shown in the design operating point for two impeller positions. The velocity measurements have been conducted in a plane perpendicular to the machine axis at half blade height and therefore contain only the ξ and the ψ components. In the discharge socket which is located at the left side of the figures the pump casing has a volume expansion in all three coordinate directions. As due to the arising optical distortions strong abnormalities for the measured velocities could be expected, in this region no velocity measurements have been accomplished. What can be clearly seen from the measurements is that a region of high velocities near the pressure side of the blade emerges and it is transported with the rotating impeller. A region with very low velocities develops behind the trailing edge of the blade and its extension is from the trailing edge to the pressure socket for the impeller position φ = 258 deg. This region increases when the impeller rotates and it also ranges from the pressure socket to the blade trailing edge for the impeller position φ = 348 deg.

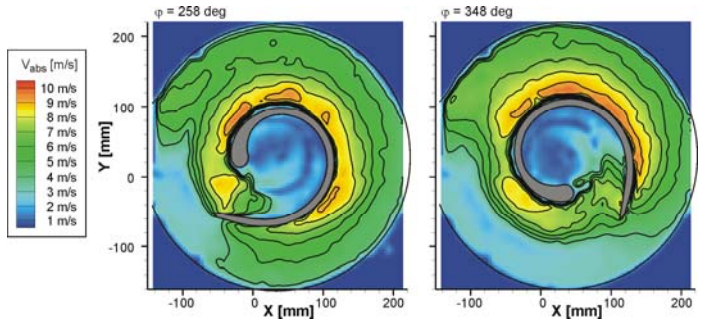

Figure 6: Measured velocity fields for 2 impeller positions (Q/Q_{des} = 100%, n = 1450 rpm)

To evaluate the time-variant velocity field in the pump in a quantitative manner and to compare the measurements to the results of the numerical simulations the measured velocity fields have been transferred to the post processor of Ansys CFX10. The interpolation of the measured velocity field to the computational grid allowed a direct comparison of measured and simulated flow fields. In figure 7 this comparison is shown for the impeller position φ=258 deg as an example. To achieve a quantitative comparison three evaluation lines were defined in

the figure, on which the comparison took place. The starting points of the lines are given in the figure as bullets.

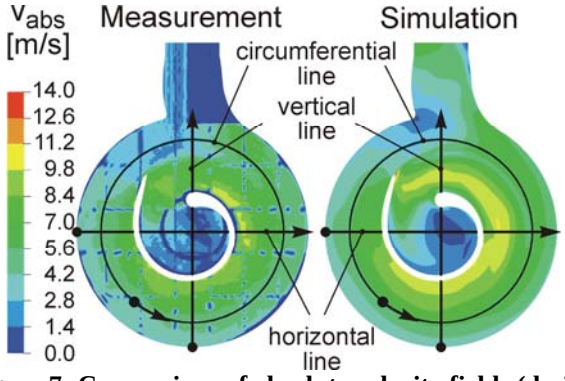

Figure 7: Comparison of absolute velocity fields (design point, φ = 258 deg, mid-span)

In figure 8 the measured and the simulated velocities are presented at the mid-span plane for the impeller positions φ=258 deg and φ=348 deg for the design operating point. The match between measurement and simulation is reasonably good. Stronger variations and a higher outlier percentage can be recognized only close to the pressure side of the blade and in the center of the pump impeller. The measured velocity distributions along the circumference of the impeller correspond very well to the numerical simulations. More about the PIV measurements in the pump can be red in [8].

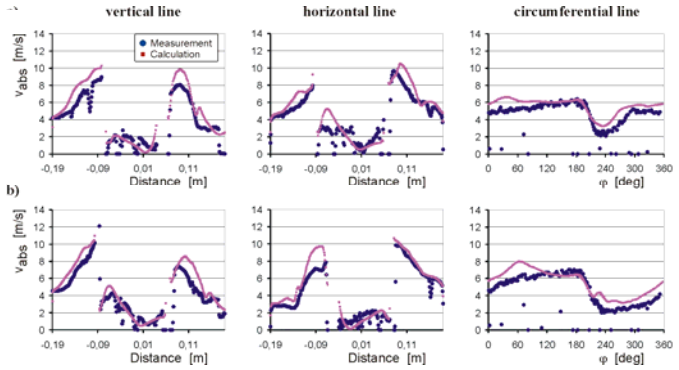

Figure 8: Quantitative comparison of measured and simulated velocities (a) φ = 258 deg, b) φ = 348 deg)

Measurements for the validation of the hydrodynamic forces obtained by numerical simulation have been conducted at the same time when the velocity measurements have been done. For this, special seats for the roller bearings of the pump shaft have been manufactured. These bearing seats allow an elastic deformation adequate to the loading of the bearings. The bearing seats consist of two rings which are connected by four bridges. The inner annulus carries the bearing and the outer annulus is mounted in the bearing housing. The bridges are used for strain measurements to give the loading at the bearings. At all bridges two strain gages have been attached at every inner side, resulting in 16 strain gages for a bearing seat. A comprehensive description of the strain gages application and the forces measurements can be taken from [9].

The setup was calibrated by different masses, which were radial attached at the shaft at half the blade height. This static calibration provided a linear relationship between the gravitational forces and the resulting voltage. Static calibration measurements have been done with the bearing seats turned in steps of 45 deg in circumferential direction for every calibration mass in order to prove the symmetry of the bearing seats and the regular attachment of the strain gages. In addition to the static calibration also dynamic calibration measurements have been performed. Although the results of the dynamic calibration showed a force orbit which had a slightly elliptic shape the magnitudes of the static calibration were confirmed by the dynamic calibration method.

In figure 9 the results of the experimental investigation of the single-blade pump are presented. The measurements shown here were phase averaged over minimum 50 impeller revolutions. The measured hydrodynamic forces which are equivalent to the loading of the bearings, have been made dimensionless by dividing the measured amounts by the reference force F_{ref} (equ. 1). The results for five operating points are shown as force orbits. As the impeller position is preserved by this method, this makes a direct comparison of the force components for all angles of impeller revolution possible. The impeller positions φ = 0, 90, 180 and 270 deg are marked in the figures by bullets. The results show a tendency of rising forces when the volume flow rate increases. The variation of the forces during one impeller revolution also becomes stronger with rising flow rate. The centers of the orbit curves for all operating points are shifted from the point of origin of the coordinate system to positive ξ-values for the annular casing.

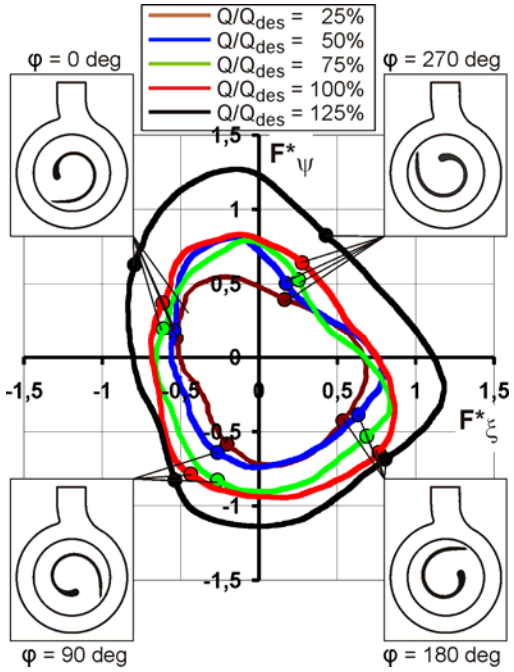

Figure 9: Measured force orbits for the annular casing with the original impeller at several operating points

In figure 10 a comparison of the experimental and the numerical (CFX10_closed_loop) obtained hydrodynamic forces is depicted for the design operation point. The ξ-components of the forces are somewhat overestimated for the complete impeller revolution by the numerical model "closed_loop", while the ψ-components meet the measurements very well.

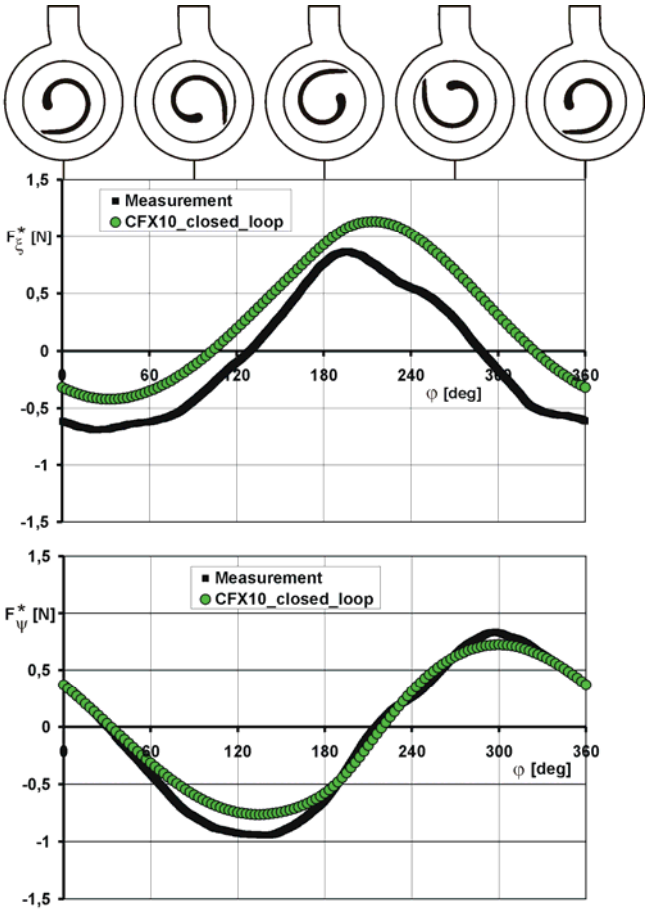

Figure 10: Comparison of numerical and experimental obtained hydrodynamic forces (Q/Q_{des} = 100%)

CONCLUSIONS

The time variance of the flow field defines the hydrodynamic behavior of single-blade sewage water pumps but is not yet completely understood. In order to contribute to the understanding of the transient flow behavior in the present contribution numerical and experimental investigations have been performed on the time-variant flow field of a single-blade pump. A qualitative and a quantitative comparison between the velocity fields obtained by numerical simulation and by measurements using an enhanced optical method (PIV-method) show a fairly good agreement in a wide range of pump operating conditions. Only for higher flow rates at certain locations inside the pump major variations occur. Despite these discrepancies at some locations and/or in special operating points the intended validation of the simulation results by the velocity measurements can be regarded as successful. A comparison of measured and calculated hydrodynamic forces show also a good qualitative agreement. Although the qualitative conformity in contrast is only good for the ψ-component the numerical simulation of the periodic flow field in the single-blade pump using commercial Navier-Stokes solvers appears to give reliable results. These numerical results can give a better insight into the transient flow structure and therefore can help to deduce directives for the design of single-blade pumps with reduced hydrodynamic forces.

Using the available numerical methods, the variation of pump design parameters in order to develop pumps having optimized hydrodynamic and mechanical loadings is feasible.

REFERENCES

[1] Agostinelli, A.; Nobles, D.; Mockridge, C. R. (1960), "An Experimental Investigation of Radial Thrust in Centrifugal Pumps", Transactions of the ASME, Journal of Engineering for Power, Vol. 82, No. 2

[2] Okamura, T. (1980), "Radial Thrust in Centrifugal Pumps with a Single-Vane-Impeller", Bulletin of the JSME 23, No. 180

[3] Aoki, M. (1984), "Instantanous Interblade Pressure Distributions and Fluctuating Radial Thrust in a Single-Blade Centrifugal Pump", Bulletin of the JSME 27, No. 233

[4] Sinha, M. and Katz, J. (2000), "Quantitative visualization of the flow in a centrifugal pump with diffuser vanes. Part I: On flow structures and turbulence", ASME Journal of Fluids Engineering, **122**, pp.97-107

[5] Wuibaut, G., Bois, G., Dupont, P., Caignaert, G., and Stanislas, M. (2002), "PIV measurements in the impeller and the vaneless diffuser of a radial flow pump in design and offdesign operating conditions," ASME Journal of Fluids Engineering, **124**, pp.791-797.

[6] Benra, F.-K., Dohmen, H. J., Sommer, M. (2005), "Periodically Unsteady Flow in a Single-Blade Centrifugal Pump - Numerical and Experimental Results", Proceedings of ASME Fluids Engineering Summer Conference, FEDSM2005-77219, Houston, Texas, USA

[7] Siekmann, H., Scheffler, T. (1997), "Unsteady Flow Field Investigations by Means of Digital Particle Image Velocimetry", Fifth Asian International Conference On Fluid Machinery, Seoul, Korea

[8] Benra, F.-K., Dohmen, H. J., Zwingenberg, M. (2006), "Comparison of Experimental and Numerical Obtained Velocity Fields in a Single-Blade Centrifugal Pump", Forum on Fluid Machinery, FEDSM2006-98351, Miami, Florida, USA

[9] Benra, F.-K., Sommer, M. (2005), "Comparison of Calculated and Measured Hydrodynamic Forces of a Centrifugal Sewage Water Pump", Proceedings of 1st International Conference on Experiments / Process / System Modeling / Simulation / Optimization, Athens, Greece